

Comparison of monotonic and cyclic pushover analyses for the near-collapse point on a mid-rise reinforced concrete framed building

Necmettin GÜNEŞ*

Department of Architecture, Sivas Cumhuriyet University, 58140, Sivas, Turkey

(Received June 22, 2020, Revised September 5, 2020, Accepted September 9, 2020)

Abstract. The near-collapse performance limit is defined as the deformation at the 20% drop of maximum base shear in the decreasing region of the pushover curve for ductile framed buildings. Although monotonic pushover analysis is preferred due to the simple application procedure, this analysis gives rise to overestimated results by neglecting the cumulative damage effects. In the present study, the acceptabilities of monotonic and cyclic pushover analysis results for the near-collapse performance limit state are determined by comparing with Incremental Dynamic Analysis (IDA) results for a 5-story Reinforced Concrete framed building. IDA is performed to obtain the collapse point, and the near-collapse drift ratios for monotonic and cyclic pushover analysis methods are obtained separately. These two alternative drift ratios are compared with the collapse drift ratio. The correlations of the maximum tensile and compression strain at the base columns and beam plastic rotations with interstory drift ratios are acquired using the nonlinear time history analysis results by the simple linear regression analyses. It is seen that these parameters are highly correlated with the interstory drift ratios, and the results reveal that the near-collapse point acquired by monotonic pushover analysis causes unacceptably high tensile and compression strains at the base columns, as well as large plastic rotations at the beams. However, it is shown that the results of cyclic pushover analysis are acceptable for the near-collapse performance limit state.

Keywords: near-collapse, collapse-prevention, performance limit states, incremental dynamic analysis, tensile strains, compression strains; monotonic pushover; cyclic pushover

1. Introduction

Damage is associated with strain and interstory drift for structural and nonstructural members, respectively (Priestley 2000). In Reinforced Concrete (RC) members, structural damage is well correlated with rebar tensile and concrete compression strains (Vidot-Vega and Kowalsky 2010). Interstory drift demand is the most used Engineering Demand Parameters (EDP), and some studies estimated drift demand using concrete compression and rebar tensile strains (Priestley 2000, Vidot-Vega and Kowalsky 2010). Also, maximum rebar strain is a crucial parameter for the assessment of the buckling of the reinforcement in the concrete columns (Moyer and Kowalsky 2003). Since concrete compression and rebar tensile strains govern nonlinear structural response, performance limit states are defined by these strain parameters (Priestley *et al.* 1996, Kowalsky 2000, TBEC 2018).

Incorporating cyclic deterioration effects in the analytical model has come into prominence to obtain accurate results by nonlinear time history (NTH) analysis. Haselton *et al.* (2016) proposed a procedure to modify the monotonic backbone curve to experimental cyclic test results for the concentrated plastic hinge modeling approach. However, energy degradation parameters are

required to adjust the RC columns cyclic behavior modeled using the finite length hinge zone model, as proposed by NIST (2010).

The ultimate deformation capacity is known as the near-collapse or collapse-prevention performance level and determined as the point of the base shear drop to 80% of maximum base shear in the decreasing region of the pushover curve for ductile framed buildings (Perus *et al.* 2006, FEMA 2009, Rejec and Fajfar 2014). However, the cumulative damage effects come into prominence during the cyclic loading, and these effects are not taken into account in the monotonic pushover analysis (Panyakapo 2014). As a result, monotonic pushover analysis causes the overestimation of strength and underestimation of deformation capacity (Panyakapo 2014). Therefore, cyclic pushover analysis is preferable to enable more precise results for first mode dominant ductile buildings and other types of structures.

Incremental dynamic analysis (IDA) has been employed to estimate the collapse performance of structures (Vamvatsikos and Cornell 2002). In this analysis, selected ground motions are scaled to the lowest intensity level, and the scale factor of each ground motion is increased in small increments until collapse occurs (Vamvatsikos and Cornell 2002, Kırçıl and Polat 2006, Ghaemian *et al.* 2020). However, using the same ground motions for all intensity levels causes conservative results due to spectral shape effects (Baker and Cornell 2006, Haselton *et al.* 2011). FEMA P695 (FEMA 2009) gives spectral shape factors to take into account the spectral shape effects, and

*Corresponding author, Assistant Professor
E-mail: ngunes@cumhuriyet.edu.tr

uncertainties can be incorporated into the fragility curve by modifying the Collapse Density Function (CDF) in FEMA P695 methodology.

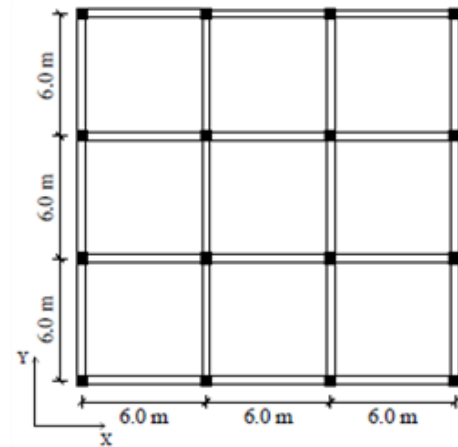
In the present study, a 5-story RC moment frame building was designed following the Turkish Earthquake and Buildings Code (TBEC 2018), and two alternative near-collapse points were obtained by performing the monotonic and cyclic pushover analyses, separately. Then, the collapse drift ratio was determined using the IDA procedure, and this ratio was compared with the drift ratio for two alternative near-collapse points. The exceedance probabilities at the Maximum Credible Earthquake (MCE) level were acquired for the drift ratios of collapse and two alternative near-collapse points using FEMA P695 methodology.

The correlations of three parameters, maximum tensile and compression strains of base columns and beam plastic rotations, with the interstory drift ratios were acquired using the IDA NTH analysis results. It was shown that the maximum tensile strain of rebars was close to the ultimate tensile strain at the drift ratio for the near-collapse point obtained by monotonic pushover analysis. Meanwhile, the maximum compression strain of the outer concrete fiber elements was over the maximum compression strain of confined concrete for the monotonic pushover analysis, and similar results were obtained for beam plastic rotations. Despite the monotonic pushover analysis results, maximum tensile and compression strains obtained using cyclic pushover analysis for the near-collapse point were significantly below the ones for the collapse point, and the flexural moment demand of beam plastic rotations was only 20% below the maximum moment of backbone curve in the decreasing region. Therefore, the near-collapse performance limit state determined using monotonic pushover analysis gave rise to overestimated interstory drift ratio as well as maximum strains and beam plastic rotations.

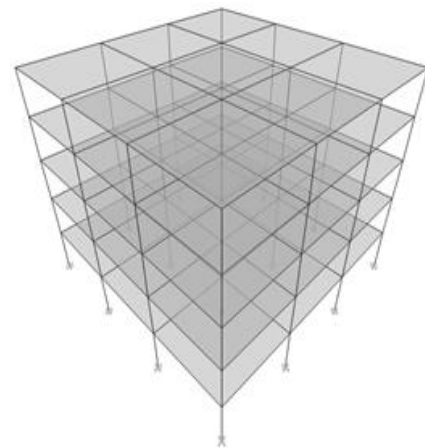
2. A case study of an RC building

A 5-story RC framed building was modeled at the site of 38.529108° latitude and 39.016981° longitudes in Elazığ, a city located in the east of Turkey. According to TBEC (2018), the site class was ZC, whose shear wave velocity for the upper 30 m was between 360-760 m/s. The geometric means of short- and long-period spectral accelerations for the design spectrum, with a return period of 475 years, were obtained from the Turkish Seismic Hazard Map (TSHM 2018) as 1.276 g and 0.431 g, respectively. In the TSHM, short and long period spectral acceleration demands were 2.363 g and 0.803 g for the MCE level at the site of interest.

The three-dimensional view and typical plan layout are shown in Fig. 1, and the other model properties are given in Table 1. In order to take into account effective flexural stiffness in accordance with TBEC (2018), the elastic stiffness modifier factors for columns, beams, and slabs were considered as 0.7, 0.35, and 0.25, respectively. The superimposed dead load was 1.5 kN/m², and the partition wall weight was 3.8 kN/m² for the exterior and 2.5 kN/m² for the interior elevations. The mid-span in X direction was



(a) Typical plan layout



(b) Three-dimensional view (ETABS 2016)

Fig. 1 Three-dimensional view and typical plan layout of the case study building

Table 1 Model properties

Story height	3.1 m
Column dimensions	0.5x0.5 m
Beam dimensions	0.35x0.60 m
Slab	0.16 m
Specified material strength	35 MPa for concrete 420 MPa for reinforcement steel

considered as a corridor. The live load was taken as 3.5 kN/m² for the corridor and 2 kN/m² for the other parts. At the roof floor, the superimposed dead load was considered at the roof floor, and the snow load was taken into account as a 1.3 kN/m² live load.

The total seismic weight of the model was obtained as 19104.36 kN by the combination of the dead load (DL) and 30% of the live load (LL). The response modification factor was taken as 8, and the design base shear ratio (V_d/W) was evaluated as 0.066. However, in the design phase, this ratio was assumed as 0.073. The design was achieved using the response spectrum analysis, and the complete quadratic combination approach was utilized to combine the mode responses using ETABS (CSI 2016) software. The first three mode periods both in the X and Y directions were 0.815 s, 0.252 s, and 0.135 s, and the related mass

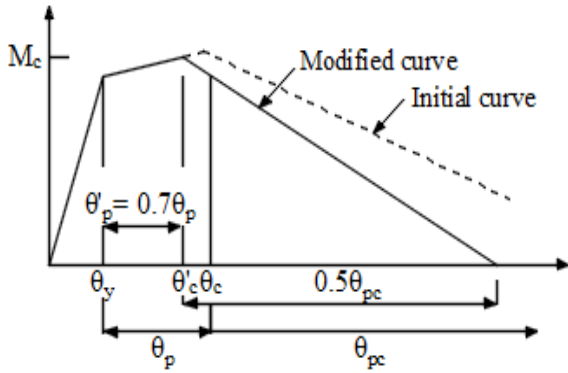


Fig. 2 Modified backbone curve (PEER/ATC 2010)

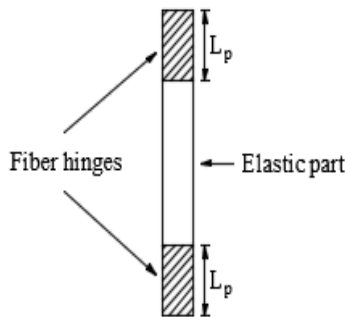


Fig. 3 Plastic hinges with fiber sections model for RC columns (NIST (2010))

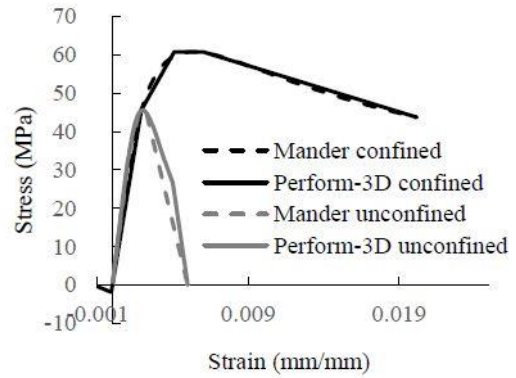
participation ratios were 0.82, 0.11, and 0.044, respectively. The RC sections design was carried out using TBEC (2018), which provides ductile behavior to prevent RC members shear failure first.

The longitudinal reinforcement ratio for columns was 1.3%, and the transverse reinforcement area (A_v) to the stirrup space (s) ratio was $0.314 \text{ cm}^2/\text{cm}$ for column confined zones. The longitudinal rebar ratios were between 0.326-0.48% for the top of the beam ends, and between 0.326-0.375% for the bottom of the beam ends. Also, the A_v/s ratio for beam confined zones was $0.157 \text{ cm}^2/\text{cm}$.

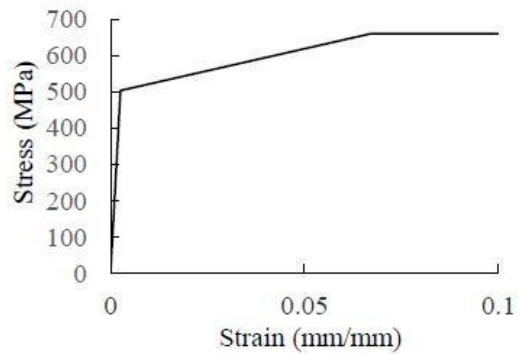
3. Nonlinear modeling

The concentrated plastic hinge approach was assumed to model the nonlinear behavior of beams, and the yielding capacity of sections was obtained using Xtract (Xtract 2010) software. Then, the pre-capping, post-capping rotation capacities, and maximum moment were obtained as given by Haselton *et al.* (2016). PEER/ATC (PEER/ATC 2010) approach was used to take into account the cyclic degradation effects for the beams, as given in Fig. 2.

The columns were modeled using NIST (NIST 2010) finite-length hinge zone model at each end with fiber elements, as illustrated in Fig. 3. The lengths of the plastic hinges were determined by the proposal of Berry and Eberhard (2008). Mander (Mander *et al.* 1989) confined and unconfined concrete models were considered with expected material properties, and the stress-strain curves for materials are given in Fig. 4. The cyclic degradation factors for



(a) Confined and unconfined concrete



(b) Reinforcement steel

Fig. 4 Stress-strain curve of materials

confined concrete were used as given in Görgülü and Taşkın (2015), and Güneş and Ulucan (2020) study was utilized for the cyclic degradation factors of unconfined concrete and reinforcement steel materials.

The shear behavior of RC members was assumed as elastic, but the shear force of each beam and column was compared with the TBEC (2018) limit, which is given in Eq. (1).

$$V_e \leq 0.85A_W \sqrt{f_{ck}} \quad (1)$$

Where the V_e , A_W and f_{ck} are shear force, effective cross-section area, and nominal strength of concrete material, respectively.

4. Cyclic pushover analysis

Ultimate deformation capacity is considered as “near-collapse” or “collapse-prevention” performance limit state (Fardis 2004, Fajfar 2007, Rejec and Fajfar 2014, Khorami *et al.* 2017), and defined as the deformation at the 20% drop of maximum base shear in the decreasing region of the pushover curve (Poljan and Fajfar, 2006, Dolsek and Fajfar 2007, FEMA 2009, Liel *et al.* 2011). Monotonic and cyclic are two alternative pushover analysis methods. However, monotonic pushover analysis underestimates the displacement capacity and overestimates the strength capacity (Koutromanos *et al.* 2011, Panyakapo 2014).

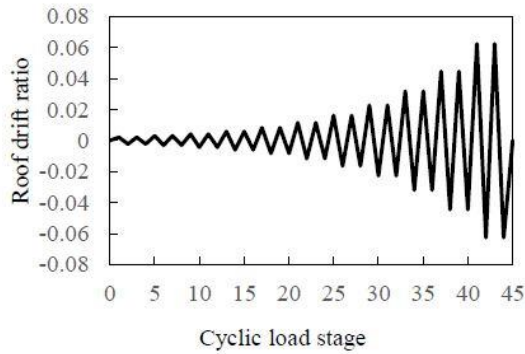


Fig. 5 Cyclic loading history

Therefore, Park (1988) proposed to consider cyclic loading effects to obtain the ultimate deformation accurately.

The cyclic loading history must be created to perform the cyclic pushover analysis. For this purpose, the FEMA 461 (FEMA 2007) cyclic loading procedure was used, in which each cyclic amplitude is repeated twice, and the next amplitude is 1.4 times of the previous amplitude. The amplitude of the roof drift ratio began with 0.00216 and finished at the 0.0625, as shown in Fig. 5.

The cyclic loading was applied to the model using PERFORM-3D (CSI 2018) software, and the results of both monotonic and cyclic pushover analysis curves are given in Fig. 6. Since the displacement-based cycling loading was employed, the base shear demand of monotonic pushover analysis was higher than that of the cyclic pushover, for the same displacement in the large deformation region. The maximum base shear force (V_{max}) was 2893.2 kN, and the design base shear force (V_d) was 1260 kN. Therefore, the overstrength factor (D) was obtained as 2.3. The ultimate drift ratios for the monotonic and cyclic pushover analyses were determined as 0.063 and 0.047, respectively. Since the near-collapse point was determined as the drift ratio at the $0.8V_{max}$ base shear in the decreasing region of pushover curves, the near-collapse drift ratio for cyclic pushover analysis was lower than that of monotonic pushover analysis due to the cumulative damage effects. The difference between these two obtained ultimate drift ratios was 25%, and to clarify this disparity, the incremental dynamic analyses were performed using FEMA P695 methodology.

5. Collapse assessment using incremental dynamic Analysis

The seismic design codes aim to provide adequate safety for the building during the extreme earthquake event (Haselton *et al.* 2011). Therefore, ASCE 7-16 (ASCE 2016) limits the collapse probability of buildings in the Risk Category I and II buildings by 10% at the MCE level. To obtain collapse probability, FEMA P695 provides a methodology based on the fitting of fragility curves using IDA results and gives 44 far-field ground motions to utilize in NTH analyses. In the present study, each FEMA P695 far-field ground motion was amplitude scaled to the first

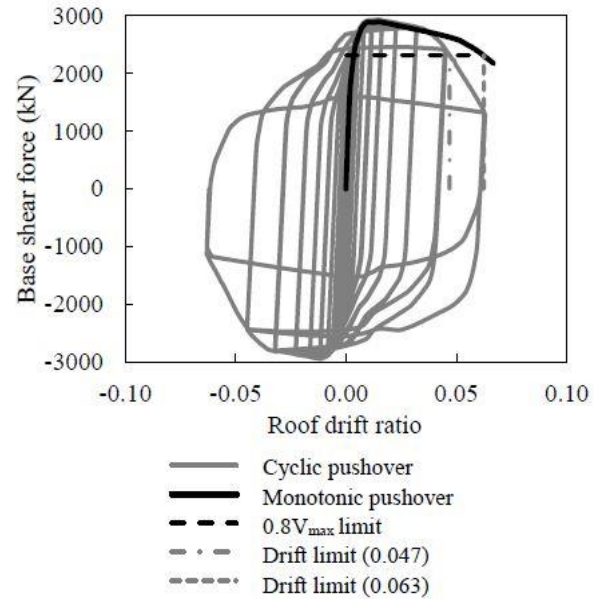


Fig. 6 Ultimate drift ratio for cyclic and monotonic pushover curves

mode spectral acceleration demand ($S_a(T_1)$) initiated at 0.05g and increased by a constant step of 0.05 g up to collapse. The relations between spectral accelerations with the maximum interstory drift ratios were obtained for each ground motion using NTH analysis results.

There are two collapse mode types. The first is the vertical collapse, and it occurs when one or more vertical members lose their gravity load capacity; the second is sidesway collapse, and it is determined as the point where the IDA curve becomes the horizontal (Zareian *et al.* 2010, Haselton *et al.* 2011, Jalilkhani *et al.* 2018). In the present study, the RC sections design was accomplished with the TBEC (2018), which enables ductile behavior. Therefore, the vertical collapse mode could only occur due to the buckling of longitudinal reinforcement of RC columns, and these effects were ignored during the NTH analyses due to the short distance between two adjacent stirrups.

In Fig. 7, 44 IDA curves were given, and each sidesway collapse point was shown on the corresponding curve. The mean and standard deviation for sidesway collapse interstory drift ratios were 0.0654 and 0.0087, respectively. The same parameters for the first mode spectral acceleration demands were 2.087 g and 1.074 g. As a result, the coefficients of variation (COV) for maximum interstory drift ratios and corresponding first mode spectral accelerations were acquired as 0.133 and 0.515, respectively. Therefore, it was seen that the mean value of the interstory drift demands of collapse points could be used for engineering judgment due to the limited deviation.

The design, test data, and model quality-related uncertainty parameters were taken from the RC special moment frame example of the FEMA P695 report. Record-to-record uncertainty and Spectral Shape Factor (SSF) were determined by the ductility demand, as given in the FEMA P695. The fragility curves of the drift ratio for two alternative near-collapse points, obtained by monotonic and

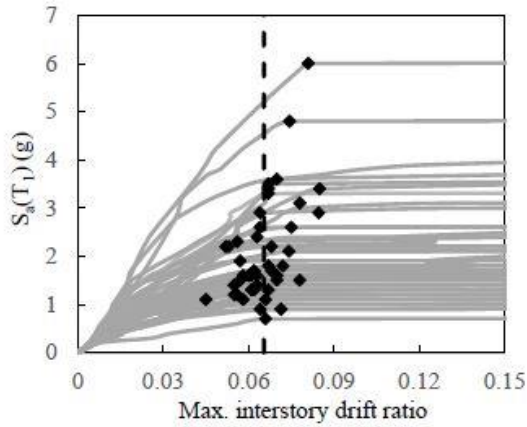


Fig. 7 IDA curves and corresponding sidesway collapse drift ratios

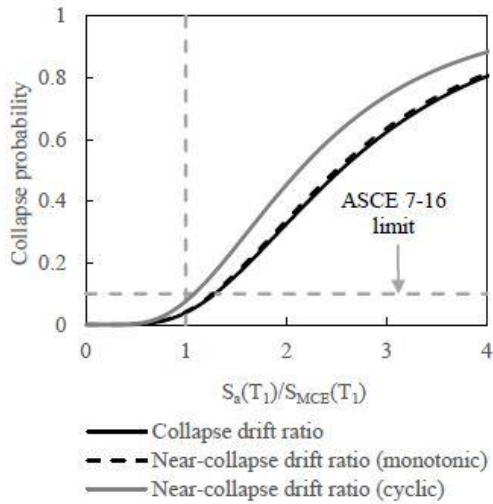


Fig. 8 Fragility curves for three different drift ratios

the cyclic pushover analyses, and that of collapse point were defined using the FEMA P695 IDA methodology. Then, the normalized fragility curves with MCE level spectral demand of the first mode period ($S_{MCE}(T_1)$) were acquired, as shown in Fig. 8. The probability of exceeding the interstory drift ratio for the near-collapse point obtained by monotonic pushover analysis was 4.23%, and the one for the sidesway collapse point was 3.93%. As expected, no significant differences were seen between both exceedance probabilities due to the closeness of their drift ratios to each other. However, the drift ratio for the near-collapse point for the cyclic pushover curve was considerably below the drift ratio for the sidesway collapse point; as a result, its exceedance probability was obtained as 7.7% at the MCE level.

6. Checking for performance levels

The performance-based design aims to predict the damage level of structures at any seismic intensity level with acceptable accuracy (Goodnight *et al.*, 2013), and structural damage is

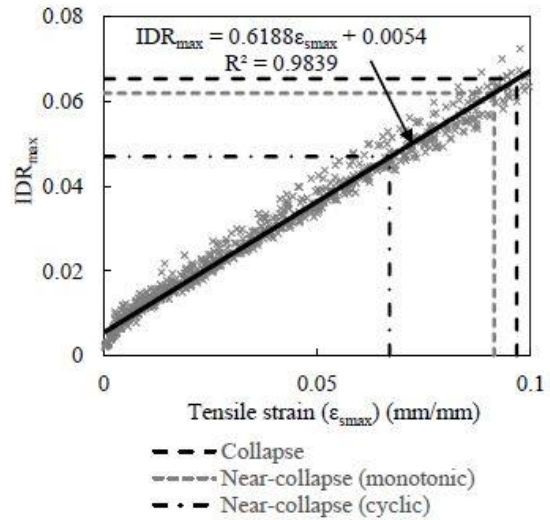


Fig. 9 The relation between IDR_{max} and base columns maximum tensile strain

interdependent with materials strain levels (Priestley 2000; Vidot-Vega and Kowalsky 2010). Therefore, Priestley (2000) limited reinforcement strain (ϵ_s) with the 0.6 times of the maximum tensile strain (ϵ_{su}) and concrete compression strain (ϵ_c) with 0.018 value. Similarly, the TBEC (2018) uses the strain limit of 0.018 concrete compression and $0.04\epsilon_{su}$ rebar tension for the upper bound of the collapse-prevention performance level. Although the interstory drift ratio is EDP to assess the global seismic performance of the buildings, there have been limited studies (Moyer and Kowalsky 2003, Priestley 2000, Vidot-Vega and Kowalsky 2010) on the estimation of drift demand using concrete compression strains, rebar tensile strains and beam plastic rotations.

In order to obtain the relation between the base columns maximum tensile strains (ϵ_{smax}) and maximum interstory drift ratios (IDR_{max}), the results of 800 NTH analyses were selected due to their rebar maximum tensile strains being below the 0.1 value and used to perform curve fitting analysis, as shown in Fig. 9

It was seen that there was a good correlation between the maximum tensile strain of the base columns and interstory drift ratios. The scattering values were curve-fitted by a simple linear function to check the interstory drift demands of sidesway collapse, monotonic and cyclic pushover analyses on the tensile strains, as given in Eq. (2).

$$IDR_{max} = 0.6188\epsilon_{smax} + 0.0054 \quad (2)$$

In this function, the corresponding maximum tensile strain for collapse drift ratio was 0.097, and for the near-collapse point drift ratio acquired by the monotonic pushover analysis was 0.093. Since these two values were close to each other, it was possible to infer that the monotonic pushover analysis overestimated the near-collapse point. On the other hand, the near-collapse point on the cyclic pushover curve created the 0.067 maximum tensile strain at the base columns, and this value was compatible with the Priestley (2000) strain limit of $0.6\epsilon_{su}$. Although the obtained relationship was based on maximum tensile strains, it was seen that there was a good correlation between the mean

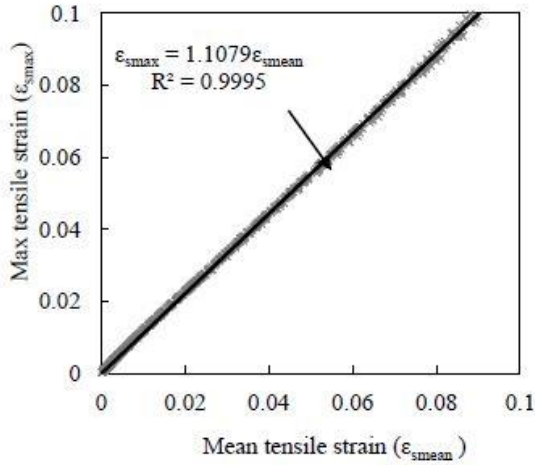


Fig. 10 The relation between the maximum and mean tensile strain of base columns

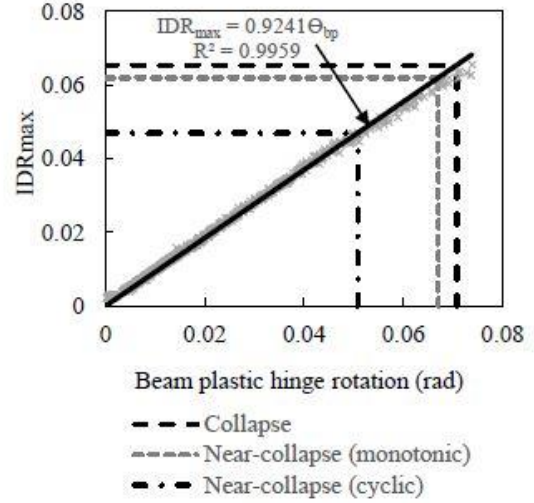


Fig. 12 The relation between interstory drift ratios and beam plastic hinge rotations

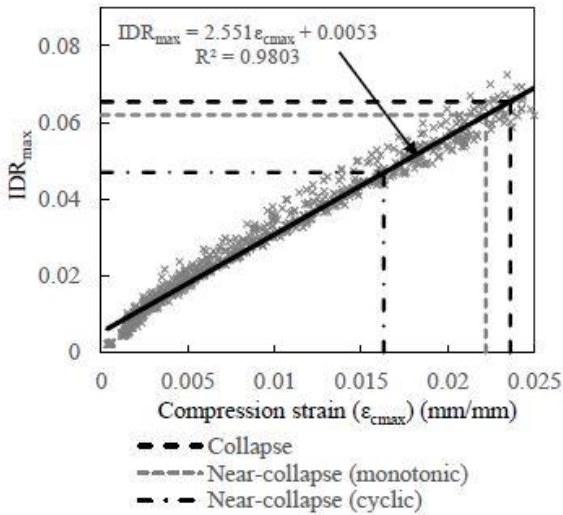


Fig. 11 The relation between maximum interstory drift ratios and base columns maximum compression strains

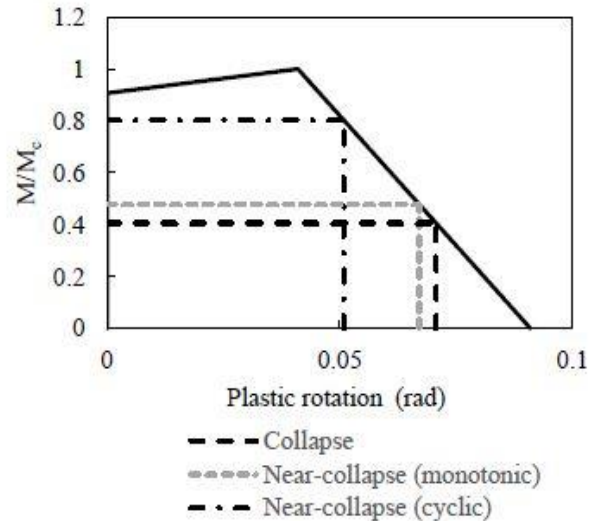


Fig. 13 Moment-rotation curve for typical beam

and maximum tensile strain of rebar outer fiber elements for base columns, as shown in Fig. 10.

The concrete compression strain is used to estimate interstory drift ratio (Priestley 2000, Vidot-Vega and Kowalsky 2010), and it is limited to 0.018 value for enabling near-collapse performance limit state (Priestley 2000; TBEC 2018). In Fig.11, the correlation between maximum concrete compression strains for base columns and maximum interstory drift ratios were illustrated for 800 NTH analysis results. Eq. (3) was obtained by the curve fitting of these results to justify the performance limits on the concrete compression strains.

$$IDR_{max} = 2.551\epsilon_{cmax} + 0.0053 \quad (3)$$

As given in the previous section, the collapse drift ratio was 0.0654, and the corresponding maximum concrete compression strain was 0.0236. According to Eq. (3), the near-collapse point obtained using monotonic pushover analysis created a 0.0226 concrete compression strain demand. This value was slightly over the limit value of maximum concrete

compression strain acquired by Mander confined concrete model, which was 0.0202, as given in Fig. 4a. Therefore, the drift demand acquired by monotonic pushover analysis should not be taken as the near-collapse performance limit state for the concrete compression strain. However, the maximum concrete compression strain for the drift ratio of the cyclic loading was obtained as 0.0163 using Eq. (3), and this value was below the allowable limit of 0.018 for near-collapse performance limit state by Priestley (2000) and TBEC (2018).

Vidot-Vega and Kowalsky (2010) showed that the beam rotations were well correlated with interstory drift ratios and just higher than the drift ratio in the plastic region. In Fig. 12, the relation between the interstory drift ratios and beam plastic hinge rotations (Θ_{bp}) were given, and it was seen that this relationship was consistent with the Vidot-Vega and Kowalsky (2010) study for the strong column-weak beam design. The maximum beam plastic rotation demand at the collapse point was 0.071 rad, whereas the maximum plastic rotation of the beams for monotonic pushover near-collapse

point was 0.068 rad. However, the same rotation for the near-collapse point assessed by cyclic pushover was 0.051 rad. These rotations and corresponding normalized flexural moments were illustrated on the moment-plastic rotation curve of a typical beam in Fig. 13. The near-collapse points for monotonic and cyclic pushover analyses created the $0.48M_c$ and $0.80M_c$ flexural moments, respectively, where the M_c was the maximum (capping) moment of the backbone curve. Likewise, the corresponding moment of collapse point was $0.41M_c$. The plastic beam rotations and their moment on the backbone curve brought to light that the results of cyclic pushover analysis could be accepted as the near-collapse point.

7. Conclusions

Near-collapse or collapse-prevention point is determined by the base shear equal to $0.8V_{max}$ in the decreasing region of the pushover curve for ductile RC framed buildings. In general, this point is defined by the monotonic pushover analysis; however, this analysis can not take into account the cumulative damage effects (Panyakapo 2014). Therefore, monotonic pushover analysis gives rise to high strength and low displacement demands compared to cyclic pushover analysis (Koutromanos *et al.* 2011, Panyakapo 2014).

In order to criticize the results of two pushover analysis methods, the near-collapse point was separately defined by monotonic and cyclic pushover analyses for a 5-story ductile RC framed building, and the results of both approaches were compared with the IDA results.

The interstory drift ratio for sidesway collapse obtained using IDA analysis was 0.0654, while the interstory drift ratios at the near-collapse point were acquired as 0.063 and 0.047 using monotonic and cyclic pushover analyses, respectively. The exceedance probabilities of all these drift ratios were below ASCE 7-16 acceptable limit, which is 10% at the MCE level.

The relationship of three parameters, maximum tensile and compression strains at the base column and beam plastic rotations, with interstory drift ratios were obtained using 800 NTH analysis results, and it was seen that all these parameters were highly correlated with interstory drift demands.

The maximum tensile strain of base columns was 0.097 and 0.093 for the sidesway collapse point and monotonic pushover near-collapse point, respectively. These values were close to the maximum tensile strain, which was 0.1 for reinforcement steel material. However, for the cyclic pushover analysis, the corresponding maximum strain for the near-collapse point was 0.067, and this value was compatible with the Priestley (2000) limit of $0.6\epsilon_{su}$.

The maximum compression strain of the base columns for the sidesway collapse point was 0.0236, and for the near-collapse point acquired using monotonic pushover analysis was 0.0226. Both of these values were over the ultimate compression strain of confined concrete, which was 0.0202. However, the maximum compression value for the near-collapse point of the cyclic pushover curve was

0.0163, and this value was 0.80 times of the maximum compression strain of the confined concrete model and below the near-collapse compression strain limit of Priestley (2000) for confined concrete, which was 0.018.

Although the maximum plastic rotation of a typical beam for sidesway collapse and monotonic pushover near-collapse points exceeded the capping plastic rotation (θ'_c) limit by 72.6% and 63.6%, respectively, the maximum plastic rotation of the typical beam was 24% larger than the θ'_c for near-collapse point of cyclic pushover analysis.

In conclusion, the near-collapse point obtained using monotonic pushover analysis was close to the sidesway collapse point for maximum tensile and compression strain of the base columns and for the beam plastic rotations. However, the results of the cyclic pushover analysis were compatible with acceptable limits. Therefore, monotonic pushover analysis overestimated the near-collapse performance limit state; on the other hand, cyclic pushover analysis results were more consistent with the assumption on strain limits.

All findings were obtained using nonlinear static and dynamic analysis results of a ductile 5-story RC framed building. Therefore, more different models with various ductility capacities are needed to be analyzed for generalizing the results.

References

- American Society of Civil Engineering (2017), Minimum design loads for buildings and other structures, ASCE 7-16, Virginia, U.S.A.
- Baker, J.W. and Cornell, C.A. (2006), "Spectral shape, epsilon and record selection", *Earthq. Eng. Struct. Dyn.*, **35**(9), 1077-1095. <https://doi.org/10.1002/eqe.571>.
- Berry, M.P. and Eberhard, M.O. (2008), *Performance modeling strategies for modern reinforced concrete bridge columns performance modeling strategies for modern reinforced concrete bridge columns*, PEER 2007/07, Pacific Earthquake Engineering Research Center. University of California, Berkeley.
- CSI (2016), *ETABS: Extended 3D Analysis of Building Systems Software*, Nonlinear Version 16.0, Computers and Structures, Inc, Berkeley, C.A.
- CSI (2018), *PERFORM-3D: Nonlinear Analysis and Performance Assessment for 3D Structures*, Version 7. Computers and Structures Inc, Berkeley, C.A.
- Disaster and Emergency Management Authority (2018), *Turkish building and earthquake code*, TBEC, Ankara, Turkey.
- Disaster and Emergency Management Authority (2018), *Turkish seismic hazard map*, TSHM, Ankara, Turkey.
- Dolsek, M. and Fajfar, P. (2007), "Simplified probabilistic seismic performance assessment of plan-asymmetric buildings", *Earthq. Eng. Struct. Dyn.*, **36**, 2021-2041. <https://doi.org/10.1002/eqe.697>.
- Fardis, M.N. (2004), "A European perspective to performance-based seismic design, assessment and retrofitting", *Proceedings of an international workshop on performance based seismic design concepts and implementation*. Pacific Earthquake Engineering Research Center College of Engineering University of California, Bled-Sloveni.
- FEMA (2007), *Interim testing protocols for determining the seismic performance characteristics of structural and nonstructural components*, FEMA 461, Federal Emergency

- Management Agency, Washington D.C., U.S.A.
- FEMA (2009), *Quantification of building seismic performance factors, FEMA P695*, Federal Emergency Management Agency, Washington D.C., U.S.A.
- Ghaemian, S., Müderrisoğlu, Z. and Yazgan, U. (2020), "The effect of finite element modeling assumptions on collapse capacity of an RC frame building", *Earthq. Struct.*, **18**(5), 555-565. <https://doi.org/10.12989/eas.2020.18.5.555>.
- Goodnight, J.C., Kowalsky, M.J. and Nau, J.M. (2013), "Effect of load history on performance limit states of circular bridge columns effect of load history on performance limit states of circular bridge columns", *J. Bridge Eng.*, **18**(12), 1383-1396. [https://doi.org/10.1061/\(ASCE\)BE.1943-5592.0000495](https://doi.org/10.1061/(ASCE)BE.1943-5592.0000495).
- Görgülü, O. and Taşkın, B. (2015), "Numerical simulation of rc infill walls under cyclic loading and calibration with widely used hysteretic models and experiments", *Bull. Earthq. Eng.*, **13**(9), 2591-2610. <https://doi.org/10.1007/s10518-015-9739-9>.
- Güneş, N. and Ulucan, Z.Ç. (2020), "Collapse probability of code-based design of a seismically isolated reinforced concrete buildings", *Bull. Earthq. Eng.* (under review)
- Haselton, C.B., Liel, A.B. and Deierlein, G.G. (2011), "Seismic collapse safety of reinforced concrete buildings. II: comparative assessment of nonductile and ductile moment frames", *ASCE J. Struct. Eng.*, **137**(4), 492-502. [https://doi.org/10.1061/\(ASCE\)ST.1943-541X.0000275](https://doi.org/10.1061/(ASCE)ST.1943-541X.0000275).
- Haselton, C.B., Baker, J.W., Liel, A.B. and Deierlein, G.G. (2011), "Accounting for ground-motion spectral shape characteristics in structural collapse assessment through an adjustment for epsilon", *J. Struct. Eng.*, **137**(3), 332-344. [https://doi.org/10.1061/\(ASCE\)ST.1943-541X.0000103](https://doi.org/10.1061/(ASCE)ST.1943-541X.0000103).
- Haselton, C.B., Liel, A.B., Taylor-Lange, S.C. and Deierlein, G.G. (2016), "Calibration of model to simulate response of reinforced concrete beam-columns to collapse", *ACI Struct. J.*, **113**(6), 1141-1152. <https://doi.org/10.14359/51689245>.
- Jalilkhani, M. and Manafpour A.R. (2018), "Evaluation of seismic collapse capacity of regular RC frames using nonlinear static procedure", *Struct. Eng. Mech.*, **68**(6), 647-660. <https://doi.org/10.12989/sem.2018.68.6.647>.
- Khorami, M., Khorami, M., Motahar, H., Alvansazyazdi, M., Shariati, M., Jalali, A. and Tahir, M.M. (2017), "Evaluation of the seismic performance of special moment frames using incremental nonlinear dynamic analysis", *Struct. Eng. Mech.*, **63**(2), 259-268. <https://doi.org/10.12989/sem.2017.63.2.25>.
- Kırçıl, M.S. and Polat, Z. (2006), "Fragility analysis of mid-rise R/C frame buildings", *Eng. Struct.*, **28**(9), 1335-1345. <https://doi.org/10.1016/j.engstruct.2006.01.004>.
- Koutromanos, I., Stavridis, A., Shing, P.B. and Willam, K. (2011), "Numerical modeling of masonry-infilled RC frames subjected to seismic loads", *Comput. Struct.*, **89**(11-12), 1026-1037. <https://doi.org/10.1016/j.compstruc.2011.01.006>.
- Kowalsky, M.J. (2000), "Deformation limit states for circular reinforced concrete bridge columns", *J. Struct. Eng.*, **126**(8), 869-878. [https://doi.org/10.1061/\(ASCE\)0733-9445\(2000\)126:8\(869\)](https://doi.org/10.1061/(ASCE)0733-9445(2000)126:8(869)).
- Liel, A.B., Haselton, C.B. and Deierlein, G.G. (2011), "Seismic collapse safety of reinforced concrete buildings. II: comparative assessment of nonductile and ductile moment frames", *J. Struct. Eng.*, **137**(4), 492-502. [https://doi.org/10.1061/\(ASCE\)ST.1943-541X.0000275](https://doi.org/10.1061/(ASCE)ST.1943-541X.0000275).
- Mander, J.B., Priestley, M.J.N. and Park, R. (1989), "Theoretical stress-strain model for confined concrete", *J. Struct. Eng.*, **114**(8), 1804-1826. [https://doi.org/10.1061/\(ASCE\)0733-9445\(1989\)114:8\(1804\)](https://doi.org/10.1061/(ASCE)0733-9445(1989)114:8(1804)).
- Moyer, M.J. and Kowalsky, M.J. (2003), "Influence of tension strain on buckling of reinforcement in concrete columns", *ACI Struct. J.*, **100**(1), 75-85. <https://doi.org/10.14359/12441>.
- NIST (2010), NEHRP Seismic Design Technical Brief No. 4: Nonlinear Structural Analysis for Seismic Design: A Guide for Practicing Engineers, NIST GCR 10-917-5, prepared by the NEHRP Consultants Joint Venture, a partnership of the Applied Technology Council and the Consortium for Universities for Research in Earthquake Engineering, for the National Institute of Standards and Technology, Gaithersburg, Maryland.
- Panagiotakos, T.B. and Fardis, M.N.F. (2003), "Performance of RC Frame Buildings designed for alternative ductility classes according to Eurocode 8", *The Fifth U.S.-Japan Workshop on Performance-Based Earthquake Engineering Methodology for Reinforced Concrete Building Structures*. Hakone, Japan, September.
- Panyakapo, P. (2014), "Cyclic pushover analysis procedure to estimate seismic demands for buildings", *Eng. Struct.*, **66**, 10-23. <https://doi.org/10.1016/j.engstruct.2014.02.001>.
- Park, R. (1988), "Ductility evaluation from laboratory and analytical testing". *Proceedings of the Ninth World Conference on Earthquake Engineering*, Tokyo-Kyoto, Japan, August.
- PEER/ATC (2010), Modeling and acceptance criteria for seismic design and analysis of tall buildings, (PEER/ATC 72-1), Applied Technology Council, Pacific Earthquake Engineering Center, Berkeley.
- Poljan, K. and Fajfar, P. (2006), "Flexural deformation capacity of rectangular RC columns determined by the CAE method", *Earthq. Eng. Struct. Dyn.*, **35**, 1453-1470. <https://doi.org/10.1002/eqe.584>.
- Priestley, M.J.N. (2000), "Performance based seismic design", *The 12th World Conference on Earthquake Engineering*, Auckland, New Zealand, February.
- Priestley, M.J.N., Seible, F. and Calvi, G.M. (1996), *Seismic Design and Retrofit of Bridges*, John Wiley and Sons, New York, U.S.A.
- Rejec, K. and Fajfar, P. (2014), "On the relation between the near collapse limit states at the element and structure level", *The Second European Conference on Earthquake Engineering and Seismology*, Istanbul, Turkey, August.
- TRC/Imbsen (2010), "XTRACT: Cross Section Analysis Software for Structural and Earthquake Engineering".
- Vamvatsikos, D. and Cornell, C.A. (2002), "Incremental dynamic analysis", *Earthq. Eng. Struct. Dyn.*, **31**(3), 491-514. <https://doi.org/10.1002/eqe.141>.
- Vidot-Vega, A.L. and Kowalsky, M.J. (2010), "Relationship between strain, curvature, and drift in reinforced concrete moment frames in support of performance-based seismic design", *ACI Structural J.*, **107**(3), 291-299. <https://doi.org/10.14359/51663694>.
- Zareian, F., Krawinkler, H., Ibarra, L. and Lignos, D. (2010), "Basic concepts and performance measures in prediction of collapse of buildings under earthquake ground motions", *Struct. Des. Tall Spec. Build.*, **19**, 167-181. <https://doi.org/10.1002/tal.546>.

AT